arXiv:1610.02173v2 [astro-ph.SR] 14 Oct 2016

The Clusters AgeS Experiment (CASE).† Variable stars in the field of the globular cluster NGC 362*

M. Rozyczka[1], I. B. Thompson[2], W. Narloch[1] W. Pych[1] and A. Schwarzenberg - Czerny[1]

[1]Nicolaus Copernicus Astronomical Center, ul. Bartycka 18, 00-716 Warsaw, Poland
e-mail: (mnr, wnarloch, pych, alex)@camk.edu.pl
[2]The Observatories of the Carnegie Institution for Science, 813 Santa Barbara Street, Pasadena, CA 91101, USA
e-mail: ian@obs.carnegiescience.edu

ABSTRACT

The field of the globular cluster NGC 362 was monitored between 1997 and 2015 in a search for variable stars. BV light curves were obtained for 151 periodic or likely periodic variables, over a hundred of which are new detections. Twelve newly detected variables are proper-motion members of the cluster: two SX Phe and two RR Lyr pulsators, one contact binary, three detached or semi-detached eclipsing binaries, and four spotted variables. The most interesting objects among these are the binary blue straggler V20 with an asymmetric light curve, and the 8.1 d semidetached binary V24 located on the red giant branch of NGC 362, which is a Chandra X-ray source. We also provide substantial new data for 24 previously known variables.

globular clusters: individual (NGC 362) – stars: variables – stars: SX Phe – blue stragglers – binaries: eclipsing

1 Introduction

The core-collapse globular cluster NGC 362 is projected against the outskirts of the Small Magellanic Cloud (SMC) at l=301°.5, b=−46°.3, in a field with a low reddening of $E(B-V)=0.05$ mag. Its core radius r_c, half-light radius r_h, tidal radius r_t, [Fe/H] index, radial velocity, heliocentric distance $d_\odot$ and galactocentric distance d_G are equal to 0′.18, 0′.82, 10′.4, -1.26, +223.5±0.5 km/s, 8.6 kpc and 9.4 kpc, respectively (Harris 1996, 2010 edition). The age of the cluster is estimated at 12.5 ± 0.5 Gyr, based on color-magnitude diagram (CMD) fitting with theoretical isochrones (Dotter et al. 2010), and its kinematics suggest an extragalactic origin (Forbes & Bridges 2010). With an exceptionally red horizontal branch and large concentration parameter (c=logr_t/r_c=1.76) NGC 362 may be regarded as a prime example of the correlation between horizontal branch morphology and central luminosity density observed among globular clusters (Dotter et al. 2010).

The cluster is a challenging target for studies with ground-based telescopes because of its distance from the Sun and high concentration. The few pre-CCD searches for variables in the field of NGC 362, summarized by Clement

†The project CASE was initiated and for long time led by our friend and tutor Janusz Kaluzny, who prematurely passed away in March 2015.

*Based on data obtained with Swope and du Pont telescopes at the Las Campanas Observatory.

et al. (2001; 2012 edition[1]) (hereafter C1-12), resulted in the detection of 16 objects. The two CCD surveys that have been performed so far (Székely et al. 2007; hereafter Sz07, and Lebzelter & Wood 2011; hereafter LW11) resulted in an additional 94 discoveries. In the whole sample of 110 variables, 56 cluster members were found by C1-12, including 35 RR Lyr and four SX Phe pulsators, three eclipsing binaries, and 14 long-period/irregular variables.

The 16 new variables belonging or probably belonging to NGC 362, and 88 new field variables presented in this contribution, are a result of the long-term photometric survey conducted within the CASE project (Kaluzny et al. 2005) using telescopes of the Las Campanas Observatory. Section 2 contains a brief report on the observations and explains the methods used to calibrate the photometry. Newly discovered variables are presented and discussed in Section 3. Section 4 contains new data on previously known variables which we consider worthy of publishing, and the paper is summarized in Section 5.

2 Observations

Our paper is based on images acquired mainly with the 1.0-m Swope telescope and the 2048×3150 SITe3 camera. The field of view was 14.8×22.8 arcmin^2 at a scale of 0.435 arcsec/pixel. Observations were obtained on 205 nights from July 7, 1997 to October 23, 2009. The same set of filters was used for all observations. A total of 3785 V-band images and 1123 B-band images were selected for analysis. The seeing ranged from $1''.14$ to $4''.3$ and $1''.28$ to $4''.07$ for V and B, respectively, with median values of $1''.67$ and $1''.8$. We also used 73 V-frames acquired in 2015 on Swope at the same resolution as before and with the same set of filters, but with the new E2V camera, and 270 frames acquired between 2001 and 2007 on the 2.5-m du Pont telescope with a field of view 8.84×8.84 arcmin^2 at a resolution of 0.259 arcsec/pixel.

The photometry was performed using an image subtraction technique implemented in the DIAPL package.[2] To reduce the effects of PSF variability, each frame was divided into 3×2 overlapping subframes. The reference frames were constructed by combining 7 images in V and 6 in B with an average seeing of $1.''26$ and $1.''33$, respectively. The light curves derived with DIAPL were converted from differential counts to magnitudes based on profile photometry and aperture corrections determined separately for each subframe of the reference frames. To extract the profile photometry from reference images and to derive aperture corrections, the standard Daophot, Allstar and Daogrow (Stetson 1987, 1990) packages were used. Profile photometry was also extracted for each individual image, enabling useful photometric measurements of stars which were overexposed on the reference frames.

2.1 Calibration

The Swope/E2V and du Pont frames were reduced and measured separately from the Swope/SITe3 frames, and the results were transformed to the SITe3 instrumental system. The photometric calibration was based on SITe3 observations of 17 standards from three Landolt fields (Landolt 1992). During the night of August 6/7, 2000 each field was observed several times, yielding a total of 39 V and B measurements at air massess $1.06 < X < 2.01$. Based on those

[1] http://www.astro.utoronto.ca/∼cclement/cat/C0100m711

[2] Available from http://users.camk.edu.pl/pych/DIAPL/index.html

measurements, the following transformations of the SITe3 photometry to the standard system were derived:

$$v - V = -2.500(1) + 0.018(1) \times (B - V)$$
$$b - B = -2.581(2) + 0.032(2) \times (B - V)$$
$$b - v = -0.078(1) + 0.951(1) \times (B - V),$$

where lower case and capital letters denote instrumental and standard magnitudes, respectively.

Crowding in the field of view resulted in enhanced blending, which in turn significantly increased the scatter of the photometric measurements in the observed magnitude range. While for the much less concentrated NGC 3201 the smallest scatter at $V = 21$ mag was 0.1 mag (Kaluzny et al. 2016), for NGC 362 it rose to 0.25 mag (Fig. 1). Fig. 2, based on the reference images, shows the CMD of the observed field. To make the figure readable, only stars with measured proper motions (Narloch et al., in preparation) are selected to serve as a background for the variables. Stars identified as proper-motion (PM) members of the cluster are shown in the right frame.

2.2 Search for variables

The search for variable stars was conducted using the AOV and AOVTRANS algorithms implemented in the TATRY code (Schwarzenberg-Czerny 1996 and 2012; Schwarzenberg-Czerny & Beaulieu 2006). We examined time-series photometric data of 51296 stars with $V < 22$ mag. The scatter of photometric mesurements was significantly offset by the large number of available frames, and as a result we were able to detect small-amplitude pulsations of SX Phe/δ Sct stars from the SMC down to about $V = 22.5$ mag. Light curves from both telescopes were searched, but due to a much smaller number of frames the data from duPont provide more information than those from Swope in only four cases. The du Pont data mainly served to make the finding charts.

We obtained light curves for most of the previously detected variables located within our field of view[3], We discovered 102 variable or likely variable stars, 16 of which are PM-members or likely PM-members of NGC 362. Several RR Lyr stars belonging to the SMC were independently discovered by Soszyński et al. (2016).

3 The new variables

Basic data for the variables discovered within this survey are given in Tables 1 and 2. The equatorial coordinates conform to the UCAC4 system (Zacharias et al. 2013) and are accurate to $0''.2$ - $0''.3$. The V-magnitudes correspond to the maximum light in the case of eclipsing binaries; in the remaining cases average magnitudes are presented. Columns 5 –7 give $B - V$ color, amplitude in the V-band, and period of variability (an empty color entry means that no B-band photometry could be extracted). A CMD of the cluster with the locations of the variables identified is shown in Fig. 3. The gray background stars are the PM-members of NGC 362 from the right frame of Fig. 2. Field objects are marked in black, those for which the PM data are missing or ambiguous in blue, and PM-members of the cluster in red.

[3]Available from the CASE archive at http://case.camk.edu.pl

3.1 Members and possible members of NGC 362

Fourteen of the newly detected periodic variables and two stars suspected of variability belong or likely belong to the cluster. The basic data for this sample are given in Table 1. Here and in subsequent Tables, magnitudes maximum light and average magnitudes are given for eclipsing binaries and remaining variables, respectively, and amplitudes ΔV refer to directly observed curves (i.e. not to the phase-binned ones). To follow the naming convention of C1-12, we begin the numbering with V17. Entries in the last column of Table 1 indicate that stars V17 – V28 are PM-members of NGC 362, whereas the membership status of VN01 – VN04 is unclear. Figs. 4a and 4b show phased light curves of all the variables from Table 1; finding charts for the stars V17 – V28 are presented in Fig. 5.

V17 and V18 are SX Phe pulsators; V17 is also a blue straggler. Although we do not have B-band data for V18, we are rather sure that it also must be located among the blue stragglers on the CMD. The large amplitude of this star, and the fact that our data seem to indicate multimode pulsations, make it a potential target for further studies. Well observed multimode pulsations would allow a determination of its mass, which in turn might provide valuable information about its origin.

V19 is a typical W UMa-type binary with a total secondary eclipse, located about 1 mag below the turnoff. Although we were able to detect low amplitude pulsations of SX Phe/δ Sct from the SMC down to $V \approx 22.5$ mag (see Table 3), we did not find any W UMa stars fainter than V19. Thus, NGC 362 provides another example of the paucity of contact binaries on the unevolved main sequences of globular clusters (Yan & Mateo 1994; Kaluzny et al. 2014). At least in cluster environments, the principal factor enabling the formation of such systems from detached binaries seems to be nuclear evolution: a contact configuration is achieved once the more massive component approaches the turnoff and starts to expand. The frequently invoked alternative, magnetic braking (e.g. Stępień & Gazeas 2012, and references therein), seems to play a minor role in the creation of W UMa stars.

V20 is an eclipsing blue straggler with an asymmetric light curve and broad minima differing by 0.65 mag in depth. From a detailed analysis of this system interesting conclusions concerning the evolution of blue stragglers might be obtained. Spectroscopic observations would be quite challenging given the orbital period of only 9.6 h, nevertheless it is worthwhile to take a spectrum just to check if lines of both components can be seen.

V21 and V22 are RRab pulsators residing in the core of NGC 362 at a projected distance $r_p \approx 0.2 r_c$ from its center. The light curve of V21 and its location about 1 mag above the horizontal branch are indicative of blending effects. In fact, in the archival HST frame 10615_01_acs_wfc_f435w_drz.fits there are two almost equally bright objects at the position of this star, separated by $\sim 0''.5$. Another example of a tight pair of RR Lyrs is Sz31 described in Sect. 4 and in the Appendix. In that case the data were sufficient to disentangle the light curves; for V21 they are unfortunately too poor. The photometry of V22 is also severely affected by blending, but most probably there is just one pulsating star in the composite image.

Broad secondary minima identify V23 as a semidetached or nearly semidetached system. Such binaries in globular clusters are potentially interesting, however low brightness and blending make this one unsuitable for a detailed analysis (in the HST frame it is located $\sim 0''.5$ from an equally bright object).

By far the most interesting object in Table 1 is the eclipsing binary V24, for which we have obtained a preliminary radial velocity curve. The nearly equal velocity amplitudes of 61.2 and 62.7 km/s and a period of 8.1 d identify this system as a pair of $\sim$0.8 $M_\odot$ stars. The shape of the light curve suggests a giant primary, most likely filling its Roche lobe, and a slightly hotter subgiant secondary. The light curve itself is extremely unstable – its only stationary parts are ingress and egress of the primary minimum. The width of the secondary minimum varies by a factor of three on a timescale of a few years, suggesting a variable flow of material between the components (perhaps an accretion disk is occasionally formed). The system coincides with the Chandra source X010322.09-705044.7, lending support to the mass transfer hypothesis. Unfortunately, the same properties that make V24 so interesting cause it to be a hard observational challenge, as several orbital periods of this system would have to be covered with high-quality photometry and spectroscopy in order to acquire a consistent picture of the mass flow and to obtain meaningful quantitative information about general physical parameters of the system.

Stars V26 and V28 belong to the red horizontal branch of NGC 362; most likely so do V25 and V27 for which we do not have B-band data. The low amplitude, slightly irregular variations of these four stars are most probably due to starspots.

VN01 is another W UMa binary. We cannot locate it on the CMD of the cluster because of the lack of B-band data. The star may, with equal probability, belong to NGC 362 (in which case it would lie on the CMD slightly above V19) or be a field object.

If the suspected variables VN02 and VN03 are members of the cluster then they reside on the extended horizontal branch (EHB). We cannot exclude such a possibility, although the physical mechanism of the variability is unclear and the EHB of NGC 362 is rather weakly populated (Moehler et al. 2000; Recio-Blanco et al. 2005).

Finally, the spotted variable VN04 may belong to NGC 362 or to the SMC. In the first case it would be located at the base of the red giant branch.

3.2 Field stars

In the observed field we detected 88 variables which, judging from their proper motions or CMD location, do not belong to NGC 362. Most of these are members of the SMC whose outskirts the cluster is projected against. 42 objects with periods longer than 0.1 d are listed in Table 2 and their light curves are shown in Figs. 6a – Figs. 6c. Several RR Lyr stars from Table 2 were independently discovered and cataloged by the OGLE team (Soszyński et al. 2016) and their catalog numbers are given in the last column. All of the 46 objects with periods shorter than 0.1 d are SX Phe or δ Sct pulsators belonging to the SMC. They are listed in Table 3 (available in its entirety from the CASE archive or in the electronic version of the paper).

Stars VN05, VN06 and VN43 have ambiguous light curves, and may be classified as W UMas or ellipsoidal variables.

VN07 can be phased with a period two times shorter than that given in Table 3, but such a period is too short for a W UMa binary (Soszyński et al. 2015). The physical cause of the variability is most probably a reflection effect.

VN08 is a genuine contact system (of two early B-type stars, judging from its color). One of the eclipses seems to be total.

The next ten entries in Table 3 are RRab stars in the SMC. Three of them

(VN10, VN11 and VN16) show clear Blazhko effect. In another two (VN13 and VN17) a weak Blazhko effect is possible, but the light curves are too noisy to identify it unambiguously.

VN19, whose proper motion indicates SMC membership, is an Algol-type system with a primary of late B-type.

The light curve of the blue star VN20 can be phased with $P = 0.793313$ d given in Table 3, but also with P=0.441828 d and P=0.306437 d. Consequently, it is an Slowly Pulsating B-Star (SPB) pulsator. It is also an SMC member.

The next 13 entries are eclipsing binaries: four Algol-type systems with ellipsoidal effect (VN22, VN23, VN26 and VN29), and nine well detached EA systems spanning a period range of 0.80 – 9.64 d.

Proper motions and/or CMD locations along the SMC red giant branch suggest that stars VN34 – VN39 are SMC members. The low amplitudes and periods from 19.5 to 29.5 d identify the first four of these as spotted red giants. The relatively higher amplitudes and longer periods of VN38 and VN39 suggest that the principal physical cause of their variability is pulsations.

VN40 is a PM-member of the SMC. Its long period and large-amplitude variations are characteristic of pulsating red giants, and the very red color ($B - V = 2.76$ mag) indicates it is a Mira variable.

VN41 is another PM-member of the SMC and it belongs to the young stellar population of that galaxy. Its color corresponds to a spectral type B3 or earlier. We did not detect any periodicity in its light curve, which caused us to mark it as a suspected variable in Fig. 3.

VN42 is located at the tip of the red giant branch of the SMC. However, we do not have proper motion for this star, and we failed to detect any red-giant type variability. It is also marked as a suspected variable in Fig. 3.

Objects VN44 – VN46 exhibit variations characteristic of red giants, but they are clearly too weak to be SMC red giants. This casts doubts on the reality of the observed variations, and we count them among suspected variables.

4 New data on known variables

We performed a cross-identification of our detected variables with the 95 stars discovered or surveyed by S07 and LW11, upon which the catalog of C1-12 is based. 22 of these were located beyond our FOV. Of the remaining stars, 26 could not be identified with any of our variables. More precisely, we did not obtain light curves of Sz18, Sz43, LW09, LW10, and LW11, and did not detect regular variability within ±10 px from the positions of Sz10, Sz24, Sz37, Sz38, Sz42, Sz47, Sz48, Sz49, Sz56, Sz61, Sz62, Sz66, Sz69, Sz76, Sz77, LW04, LW05, and LW12 (all star names in this Section and in the Appendix are taken from C1-12). Variability detected within ±10 px from the positions of Sz41 and Sz59 turned out to be spurious (induced by blending with neighboring variables Sz57 in the first case, and Sz35 in the second). Finally, the light curve of the only variable object within ±10 px from the position of Sz25 was too poor for a detailed analysis (we are sure, however, it is not a Cepheid curve as suggested by S07). For the 24 variables listed in Table 4 our photometry provided new information which we consider worthy of publishing. The light curves for these objects are shown in Figs. 7a and 7b.

Sz09: The eclipses differ in depth by ∼0.05 mag, indicating nearly equal temperatures for the components. NGC 362 has $E(B-V) = 0.05$ mag (H96-10). Assuming the same reddening for Sz09 (note this is a lower estimate, since

the binary must be more distant from the Sun than the cluster), we obtain $E(B-V)_o \leq -0.31$ mag, and $T_e \geq 36,000$ K characteristic of O-type stars. The shape of the light curve indicates that at least one component is severely tidally distorted. Since the light curve is smooth and stable, and no period changes have been observed, any mass transfer between the components must be very low. Most probably, Sz09 is a detached system whose (slightly) more massive component has just left or is about to leave the main sequence.

Sz12: S07 had only one night of data available and they could not measure a complete light curve. We obtained a complete light curve of a typical RRab star, whose CMD-location clearly suggests SMC membership.

Sz17: We obtained a multiseason light curve and found that it is generally stable, with $\sim$0.05 mag fluctuations around the mean. The period is slightly shorter than estimated by S07 and stable. We confirm the star is a red giant belonging to the cluster.

Sz19: The star is located at a projected distance $r_p \approx 0.5 r_t$ from cluster center, but both its CMD-location and proper motion clearly indicate that it belongs to the SMC. The multiseason light curve has an amplitude of nearly 1.8 mag, and a stable period of $\sim$0.5 yr.

Sz20: This blue straggler is the only star for which we do not confirm the type of variability suggested by S07. According to our data it is a W UMa-type binary rather than an SX Phe pulsator. Since our coordinates differ by $1''.5$ from the S07 values we cannot exclude a misidentification. However we did not find any SX Phe-type variability within ± 10 px from the position of Sz20.

Sz28: For this field W UMa-type variable we provide a much better phase coverage than that of S07.

Sz31: On the archival HST frame 10615_01_acs_wfc_f435w_drz.fits Sz31 this object splits into two stars of nearly equal brightness with a separation of $0''.7$ (S07 found a separation of only $0''.16$, and suggested the two stars may be physically related). Upon disentangling the combined light curve we obtained periods of 0.53 d and 0.56 d, and derived two separate complete RRab light curves. The details of the analysis are given in the Appendix. Based on the CMD-location and $r_p \approx 0.1 r_t$, both the components of the blend are very likely members of NGC 362.

Sz32: The star, tentatively classified by S07 as EA, has in fact a nearly perfectly sinusoidal light curve whose physical origin is difficult to establish. C1-12 counted Sz32 as a cluster member. However, it is too dim to be an RRc pulsator belonging to NGC 362; its location at $r_p \approx r_t$ also suggests that is a field star.

Sz33: S07 published an incomplete light curve. We show this cluster member to be an RRab pulsator with a slightly ($\sim$0.1 mag) varying amplitude, but with an otherwise stable light curve.

Sz34: Same remarks as for Sz33, except that the amplitude of this star does not vary. The light curve shown in Fig. 7a is derived from du Pont data. Its counterpart from the Swope data has a larger scatter, but no amplitude modulation can be observed.

Sz36: We confirm the cluster membership of this variable red giant, as suggested by C1-12. The multiperiodic light curve can be reasonably phased with $P = 238.1$ d, but also with 26.43, 39.62 and 46.50 d, the latter value being close to the 45 d period given by C1-12.

Sz40: For this star we observe a pronounced Blazhko effect which cannot be seen in the S07 data because of insufficient time-coverage. Sz40 is a confirmed member of NGC 362.

Sz44: The light curve of S07 is incomplete and distorted. Our data show that Sz44 is an RRab pulsator with a stable light curve. With $r_p \approx 0.02 r_t$ and a CMD location among the NGC 362 RR Lyr stars it is a confirmed cluster member.

Sz45: Same remarks as for S44, the only difference being a weaker Blazhko effect.

Sz50: S07 published a smooth RRab-like light curve, but they remarked that it was strongly variable. At first glance, our light curve in Fig. 7b looks somewhat chaotic. However, a careful analysis (detailed in the Appendix) allowed us to conclude that Sz50 is a double-mode RRd pulsator showing the Blazhko effect. Like Sz44, Sz50 is a firm cluster member.

Sz51: This star, for which S07 do not provide the light curve, resides at the very tip of the red giant branch of the cluster. Both its proper motion and location at $r_p \approx 0.03 r_t$ strongly speak for NGC 362 membership.

Sz55, Sz64 and Sz65: In these three cases our data show Blazhko effects of various strengths which were not be observed by S07 due to insufficient time coverage.

Sz68: For this star we have detected a significantly more complicated Blazhko effect than those reported by S07.

Sz70: S07 list this object among stars with no period and secure classification. We find it to be an RRab pulsator, probably with a Blazhko effect. At $V \sim 19$ mag it is most likely an SMC member.

V002: Our sampling of the light curve is much denser than that of LW11; we also find the period to be 108 d rather than 105 d. Our data indicate that V002 is a PM-member of NGC 362.

LW03: This red giant is a cluster member. We find its period to be much longer than that reported by LW11 based on few measurements (174 d vs. 51 d).

LW08: Another red giant belonging to the cluster. The dominant period seems to be 187 d rather than 63 d suggested by LW11. Also, we do not see their 954 d periodicity.

5 Summary

We have conducted an 18-year long photometric survey of the NGC 362 field in a search for variable stars. A total of 100 variables plus four suspected variables were discovered, and multiseasonal light curves were compiled for another 46 variables that had been known before. Periods were obtained for all observed variables except VN41 and VN42 which appear to vary on a timescale longer than our time base. Four new eclipsing binaries and two pulsating stars of SX Phe-type were found to be PM-members of NGC 362. The most interesting, but at the same time rather challenging objects for follow-up studies are the binary blue straggler V20 with an asymmetric light curve, and the 8.1 d semidetached binary V24 located at the red giant branch of the cluster and coinciding with a Chandra X-ray source. The latter system is a pair of ~ 0.8 $M_\odot$ stars: the giant primary most likely filling its Roche lobe and a slightly hotter subgiant secondary. The width of the secondary minimum varies by a factor of three on a timescale of a few years, suggesting a variable flow of matter between the components.

We also provide substantial new data on 24 of the variables cataloged by C1-12. Deserving further study are six RR Lyras with Blazhko effects; in par-

ticular the multimode star Sz50 whose lightcurve can dramatically change on a timescale of a few weeks. Finally, we collected a sample of 42 SX Phe/δ Sct pulsators belonging to the SMC.

Acknowledgements. WN, WP and MR were partly supported by the grant DEC-2012/05/B/ST9/03931 from the Polish National Science Center. We thank Grzegorz Pojmański for the lc code which vastly facilitated the work with light curves. This paper is partly based on data obtained from the Mikulski Archive for Space Telescopes (MAST). STScI is operated by AURA, Inc., under NASA contract NAS5-26555. Support for MAST for non-HST data is provided by the NASA Office of Space Science via grant NNX09AF08G and by other grants and contracts.

REFERENCES

Clement, C. M., Muzzin, A., Dufton, Q., Ponnampalam, T., Wang, J. et al. 2001, *Astron. J.*, **122**, 2587 (C1-12).
Dotter, A., Sarajedini, A., Anderson, J., Aparicio, A., Bedin, L. R. et al. 2010, *ApJ*, **708**, 698.
Forbes, D. A., and Bridges, T. MNRAS, *2010*, **404**, 1203.
Harris, W.E. 1996, *Astron. J.*, **112**, 1487.
Kaluzny, J., Rozyczka, M., Thompson, I. B., Narloch, W., Mazur, B. et al. 2016, *Acta Astron.*, **66**, 31.
Kaluzny, J., Thompson, I. B., Krzeminski, W., Preston, G. W., Pych, W. et al. 2005, *Stellar Astrophysics with the Worlds Largest Telescopes, AIP Conf. Proc.*, **752**, 70.
Kaluzny, J., Thompson, I. B., Rozyczka, M., Pych, W., and Narloch, W. 2014, *Acta Astron.*, **64**, 309.
Landolt, A. 1992, *Astron. J.*, **104**, 372.
Lebzelter, T., and Wood, P. R. 2011, *Astron. Astrophys.*, **529**, A137 (LW11).
Moehler, S., Landsman, W. B., and Dorman, B. 2000, *Astron. Astrophys.*, **361**, 937.
Moskalik, P. 2013, *Precision Asteroseismology, IAU Symposium*, **301**, 249.
Recio-Blanco, A., Piotto, G., De Angeli, F., Cassisi, S., Riello, M. et al. 2005, *Astron. Astrophys.*, **432**, 851.
Schwarzenberg-Czerny, A. 1996, *Astrophys. J. Letters*, **460**, L107.
Schwarzenberg-Czerny, A. 2012, *New Horizons in Time-Domain Astronomy, IAU Symposium*, **285**, 81.
Schwarzenberg-Czerny A., and Beaulieu, J.-Ph. 2006, *MNRAS*, **365**, 165.
Soszyński, I., Stępień, K., Pilecki, B., Mróz, P., Udalski, A. et al. 2015, *Acta Astron.*, **65**, 39.
Soszyński, I., Udalski, A., Szymański, M. K., Wyrzykowski, Ł., Ulaczyk, K. et al. 2016, *Acta Astron.*, **66**, 131.
Stępień, K., and Gazeas, K. 2012, *Acta Astron.*, **62**, 153.
Stetson, P. B. 1987, *P.A.S.P.*, **99**, 191.
Stetson, P. B. 1990, *P.A.S.P.*, **102**, 932.
Székely, P., Kiss, L. L., Jackson, R., Derekas, A., Csák, B, and K. Szatmáry, K. 2007, *Astron. Astrophys.*, **463**, 589 (S07).
Szegö, G. 1939, *Orthogonal polynomials*, **Colloq. Publ. Amer. Math. Soc. 23**, .
Yan, L., and Mateo, M. 1994, *Astron. J.*, **108**, 1810.
Zacharias, N., Finch, C. T., Girard, T. M., Henden, A., Bartlett, J. L. et al. 2013, *Astron. J.*, **145**, 44.
Zloczewski, K., Kaluzny, J., Rozyczka, M., Krzeminski, W., and Mazur, B. 2012, *Acta Astron.*, **62**, 357.

Appendix: The complex light curves of Sz31, Sz50 and Sz55

6.1 Light curve decomposition

A first glance at light curves of some RR Lyrae stars in NGC 362 reveals evidence of multiple mode pulsation and/or modulation of amplitude or shape of the light curve. To investigate this behavior in more detail we employed a new code, Baca, for prewhitening and decomposition of a light curve into individual modes. In a prologue, data are normalized by subtraction from observation times of their median, treated as epoch of observations and by replacing observation errors with their inverses, treated as square root of weights. Provision exists to flag observation as invalid. Next, time sampling is analyzed to determine optimum frequency resolution Nyquist frequency range from median of observation intervals. With frequency grid fixed we start core calculation by finding consecutive frequencies from periodogram peak of prewhitened data. Prewhitening is performed at each stage by fitting the original data with the current model by Newton-Raphson nonlinear-least squares (NLSQ) iterations involving adjustments to amplitudes and frequencies, and subtracting it from the observations. Next, an AOV periodogram of prewhitened data is calculated by orthogonal projection of Szegö trigonometric polynomials, its peak frequency is found by parabola fitting, and the result is appended it to the current model (Schwarzenberg-Czerny 1996, 2012). We perform a total decomposition of the light curve by recursively repeating this procedure till no oscillations exceed noise. In the process, dependent frequencies are identified and tied to their base frequencies. In the epilogue it is possible to inspect light curves of individual modes by prewhitening the observations with a subset of frequencies and folding the result with the frequency of interest.

6.2 Star Sz31

Preliminary periodograms revealed two principal frequencies. Their final values $f_1 = 1.885492451 \pm 0.000000054$ c/d and $f_2 = 1.789493550 \pm 0.000000055$ c/d were obtained by prewhitening the data with a trigonometric series up to 15 harmonics of the first frequency, and, subsequently, fitting a Szegö series with frequency adjustment. To separate the light curves, we first converted magnitudes to fluxes. Next, for fixed frequencies we fitted the fluxes with the sum of two Szegö series of frequencies f_1 and f_2 with 21 terms each. No clipping was applied. The final light curves plotted in the right panel of Fig. 8 were obtained by adding half of the flux residuals to each model light curve, and then converting to magnitudes. The residuals show a mild systematic trend during the minima of star 2. In our opinion, this may constitute cross-talk from star 1 resulting from image subtraction photometry for single PSF position centered closer to star 1 than to star 2.

6.3 Star Sz50

We analyzed separately two sets of observations containing most of the data. Each of them consisted of two observing seasons, and spanned slightly over a year: Set 1 with 1028 points from HJD 3917 till HJD 4362, and Set 2 with 422 points from HJD 4698 till HJD 4699. The two strongest oscillations in Set 1 have amplitudes of 0.117 and 0.083 mag, and frequencies $f_0 = 2.0483 \pm 0.0010$ and

$f_1 = 2.8048 \pm 0.0025$ c/d, respectively. In Set 2 the strongest peak corresponds to $2f_0$ harmonic of amplitude 0.083 mag, while the second and third ones with amplitudes of 0.066 and 0.051 mag - to $f_0 + 1$ c/d alias, and to f_1, respectively. The ratio $f_0/f_1 = 0.73$ is consistent with Petersen diagrams of fundamental and first overtone bimodal RR Lyr (see e.g. Moskalik 2013). The frequencies and their errors quoted above were derived from the analysis of harmonic and combination peaks at higher frequencies corresponding to signatures [1,0], [0,1], [2,0], [1,0], [1,1], [3,0], [2,1], [3,1], [4,0] in Set 1 and [2,0], [1,0], [0,1], [1,1], [4,0] in Set 2, where the first and second digit is harmonic and base frequency number, respectively. Solving by least squares for Set 1 and Set 2 independently, we obtained two values of f_0 and two of f_1 (in each case consistent within less than 1.5σ) which were subsequently averaged. A cautionary remark is due here: given that no season spans more than 70 days, we cannot completely exclude year aliasses ± 0.0027 c/d of base frequencies. However, base frequencies derived from harmonics are less affected.

Two more facts are noteworthy. First, at amplitudes of 0.075 and 0.083 mag the $2f_0$ harmonic is strong in Set 1 and dominant in Set 2, making an impression of period halving. Second, in Set 1 there is evidence of a weak oscillation with amplitude 0.019 mag and frequency 1.0120 c/d - a possible subharmonic $f_0/2$. The amplitude of this sub-harmonic in the whole data is even stronger, at 0.030 mag. Additionally, our data yield strong evidence of amplitude modulation of principal modes on time scales over 100 days. In four panels of Fig. 9 we plot light curves phased with frequencies f_0 and f_1 for Set 1, and $2f_0$ and f_1 for Set 2 after prewhitening of all other modes. Appreciable changes of their amplitude and shape may indicate a Blazhko modulation. A further hint towards the Blazhko modulation is our inability to remove power near f_0 by fitting just one sinusoid to Set 1 data: two components spaced by 0.010 c/d were needed, whereas in case of window-function ghosts removing the stronger component usually removes the fainter ones, too. Similarly, three components were needed to remove f_0 and two components to remove f_1 from the whole dataset. Thus, there is some evidence of a long-term frequency modulation.

Apart from that Set 1 yields no unexplained oscillations with amplitudes exceeding 0.01 mag. In Set 2, amplitudes of ≈ 0.02 mag appear at frequencies 1.77 and 0.69 c/d, close to $f_0/3$. However this data set is poorer, consisting of runs not exceeding 40 d, hence we refrain from further discussion.

6.4 Star Sz55

Analysis of this star reveals presence of one pulsation mode at a frequency $f_0 = 1.96185 \pm 41$ c/d together with its multiple harmonics and their day aliasses. Apart from that, up to frequency of 35 c/d no unrelated oscillations with amplitudes over 0.02 mag can be detected. Similarly as in the case of Sz50, we derived the final value of the period by averaging results from three data sets from HJD ranges given in Table 5. Actually, for this purpose we used $5f_0$ harmonics present in all data sets, as their relative error was a factor of ~ 5 less than that for f_0 itself. Assuming a coherence throughout the whole data set would be risky, given pronounced changes of the shape of the light curve. However, the consistency of results speaks for period stability and correct cycle count, while the scatter of individual values yields a robust estimate of the error.
Up to 10 harmonics reveal amplitudes exceeding 0.01 mag, though on occasions the strongest peaks correspond to their ± 1 and ± 2 c/d aliasses. This said, it must be stressed that their amplitudes are anything but stable, revealing

between seasons changes of up to factor 2 both in absolute and relative sense. The corresponding changes of light curve shape are illustrated in three panels of Fig. 10. However, the time scale of this modulation likely is of a large fraction of a year (otherwise the peaks in our periodogram would reveal broadening or subcomponents). Due to large seasonal gaps we are unable to check this long-term modulation for periodicity, but a first guess would be we are observing Blazhko-type modulation on a time scale of a few hundred days.

Table 1: Basic data of newly discovered variables belonging or likely belonging to NGC 362

ID	RA [deg]	DEC [deg]	V [mag]	$B-V$ [mag]	Δ_V [mag]	Period [d]	Type[a] Remarks[b]	Mem[c]
V17	15.695623	-70.762892	18.168	0.255	0.015	0.034562	SX; BS	Y
V18	15.825319	-70.842839	17.671		0.451	0.067906	SX	Y
V19	15.639185	-70.784220	19.673	0.559	0.449	0.231436	EW	Y
V20	15.831187	-70.844957	17.251	0.229	0.737	0.402175	EB/EW; BS	Y
V21	15.819295	-70.847854	14.550	0.393	0.460	0.520397	RRab	Y
V22	15.801621	-70.846397	15.888	0.248	0.236	0.566332	RRab	Y
V23	15.732048	-70.852705	18.385	0.600	0.210	0.920841	EA	Y
V24	15.842032	-70.845761	16.272	0.817	0.266	8.140462	EA; RG; X	Y
V25	15.893542	-70.899521	15.727		0.681	12.51458	Sp	Y
V26	15.659105	-70.914325	15.495	0.663	0.020	14.72401	Sp	Y
V27	15.875219	-70.922811	15.079	0.869	0.091	15.05222	Sp	Y
V28	15.669002	-70.816794	15.529	0.567	0.028	24.30491	Sp	Y
VN01	15.767435	-70.841165	18.811		0.840	0.261285	EW	U
VN02	15.567987	-70.861797	16.692	-0.115	0.111	0.764585	*s*	U
VN03	15.698946	-70.668651	16.037	-0.043	0.131	1.081190	*s*	U
VN04	15.485683	-70.963615	18.255		0.247	13.45729	Sp	U

[a] EA - detached eclipsing binary, EB - close eclipsing binary, EW - contact binary, Ell - Ellipsoidal variable, Sp - spotted variable, RRab - RRab pulsator, SX - SX Phe pulsator, *s* - suspected variable.
[b] BS- blue straggler, RG - red giant, X - X-ray source.
[c] Membership status: Y - member, U - no data or data ambiguous.

Table 2: Basic data of field variables identified within the present survey

ID	RA [deg]	DEC [deg]	V [mag]	$B-V$ [mag]	Δ_V [mag]	Period [d]	Type[a]	OGLE ID[b]
VN05	15.835164	-70.821843	19.754	0.708	0.268	0.229394	EW	
VN06	15.701709	-70.840557	19.735	0.656	0.362	0.261982	EW	
VN07	16.101429	-70.757218	18.091	1.107	0.055	0.337148	Ell?	
VN08	15.905190	-70.672751	19.346	-0.150	0.632	0.472937	EW	
VN09	15.926041	-70.758607	19.579	0.339	0.937	0.547801	RRab	4642
VN10	15.508883	-70.840514	19.781	0.323	0.845	0.595133	RRab	4560
VN11	15.835365	-70.804176	19.645	0.361	0.779	0.617199	RRab	4625
VN12	16.146925	-70.924962	19.531	0.350	0.644	0.620290	RRab	4669
VN13	15.752016	-70.808638	19.333	0.401	0.485	0.624751	RRab	4601
VN14	15.789838	-70.755247	19.652	0.306	0.584	0.631775	RRab	4614
VN15	15.745504	-70.661926	19.896	0.371	0.531	0.634066	RRab	4599
VN16	15.541113	-70.976611	19.456	0.376	0.429	0.648357	RRab	
VN17	16.169725	-70.819698	19.691	0.382	0.505	0.650213	RRab	4672
VN18	16.189086	-70.870573	19.619	0.380	0.671	0.689559	RRab	4673
VN19	15.472769	-70.890452	19.591	-0.017	0.658	0.707474	EA	
VN20	15.645727	-70.920385	17.988	-0.045	0.103	0.793313	SPB	
VN21	15.552856	-70.966519	21.512	0.279	0.960	0.795833	EA	
VN22	15.805797	-70.871584	19.040	0.000	0.247	0.874733	EA	
VN23	15.660924	-70.836421	18.933	-0.196	0.440	1.039676	EA	
VN24	15.749289	-70.776986	21.399	0.447	0.833	1.083923	EA	
VN25	15.784002	-70.680881	18.776	-0.074	0.321	1.213690	EA	
VN26	16.008099	-71.015307	19.366	0.076	0.235	1.358603	EA	
VN27	15.698910	-70.823079	18.852	0.038	0.161	3.099988	EA	
VN28	15.463015	-70.889363	20.444	0.238	0.616	3.576705	EA	
VN29	15.849144	-70.959040	17.998	-0.103	0.100	4.110868	EA	
VN30	15.876971	-70.675557	20.458	0.010	0.488	4.400843	EA	
VN31	16.047540	-70.756549	21.745	0.658	1.033	4.415142	EA	
VN32	15.746235	-70.900027	20.989	0.027	0.788	5.782922	EA	
VN33	15.729061	-71.027554	18.437	-0.058	0.198	9.640647	EA	
VN34	15.545848	-70.944889	16.421	1.486	0.054	15.05222	Sp; RG	
VN35	15.737894	-70.984428	15.550	1.424	0.029	19.46125	Sp; RG	
VN36	15.819203	-70.922276	17.632	1.164	0.058	24.30491	Sp; RG	
VN37	16.041693	-70.753661	18.754	0.910	0.090	29.54246	Sp; RG	
VN38	15.692691	-70.677675	16.294	1.821	0.249	55.94843	Sp?; RG	
VN39	16.019315	-70.945663	16.705	1.600	0.184	62.95116	Sp?; RG	
VN40	15.956149	-70.730158	16.950	2.764	1.060	262.2845	LPV; RG	
VN41	15.912747	-70.819997	16.966	-0.148	0.167	4500.000[c]	*s*	
VN42	16.035620	-70.976718	16.240	1.783	0.285	4600.000[c]	RG; *s*	
VN43	16.170235	-70.884000	21.037	0.312	0.434	0.172275	EW	
VN44	16.151624	-70.732550	22.301		0.553	18.71347	*s*	
VN45	15.577582	-70.876860	22.829		1.073	27.33038	*s*	
VN46	15.833286	-70.905513	21.149		1.110	107.8565	*s*	

[a] EA - detached eclipsing binary, EB - close eclipsing binary, EW - contact binary, Ell - Ellipsoidal variable, Sp - spotted variable, RRab - RRab pulsator, SPB - SPB pulsator, LPV - long period variable, RG - red giant, *s* - suspected variable.
[b] From Soszyński et al. (2016).
[c] Time-span between the first and the last observation.

Table 3: Basic data of 46 SX Phe/δ Sct pulsators from the SMC identified within the present survey*

ID	RA [deg]	DEC [deg]	V [mag]	$B-V$ [mag]	Period [d]
VN47	16.179903	-71.005473	22.967		0.031072
VN48	16.075408	-70.925832	22.309	0.122	0.039332
...	...	...	...	...	...
VN91	15.638799	-70.962703	21.615	0.239	0.074687
VN92	16.124508	-70.804743	21.767	0.118	0.077352

* Available in its entirety from the CASE archive or in the electronic version of the paper.

Table 4: Basic data of S07 and LW11 variables for which important new information is provided

ID[a]	RA [deg]	DEC [deg]	V [mag]	$B-V$ [mag]	Δ_V [mag]	Period [d]	Type[b] Remarks[c]	Mem[d]
Sz09	15.491038	-70.991094	15.837	-0.262	0.270	1.252792	EA	N
Sz12	15.500430	-70.983710	19.686	0.351	0.589	0.697098	RRab	N
Sz17	15.658535	-70.856023	13.391	1.232	0.156	67.73800	LPV; RG	Y
Sz19	15.666372	-70.774557	17.343	3.437	1.796	187.3436	LPV	N
Sz20	15.675416	-70.783423	17.567	0.147	0.124	0.356646	EW; BS	Y
Sz28	15.747879	-70.987791	18.969	0.825	0.535	0.238010	EW	N
Sz31	15.768227	-70.855610	14.751	0.310	0.707	0.530364	RRab	Y
Sz32	15.771615	-71.001746	17.045	0.263	0.148	0.585562	Ell?	U
Sz33	15.772487	-70.850987	15.540	0.268	0.613	0.644707	RRab; Bl	Y
Sz34	15.780658	-70.848124	15.414	0.178	0.549	0.643308	RRab	Y
Sz36	15.782375	-70.829589	12.766	1.415	0.164	237.7636	LPV; RG	Y
Sz40	15.788274	-70.866926	15.535	0.322	0.983	0.517682	RRab; Bl	Y
Sz44	15.798804	-70.846290	15.206	0.266	0.751	0.549218	RRab	Y
Sz45	15.799041	-70.847472	15.005	0.316	0.785	0.514701	RRab; Bl	U
Sz50	15.810568	-70.864042	15.245	0.410	0.373	0.489414	RRd; Bl	Y
Sz51	15.812784	-70.842350	11.695	2.187	0.758	138.0398	LPV; RG	Y
Sz55	15.823751	-70.838109	15.348	0.391	0.921	0.509843	RRab; Bl	Y
Sz64	15.845882	-70.843214	15.327	0.298	0.634	0.607315	RRab; Bl	Y
Sz65	15.851014	-70.845423	15.417	0.414	0.268	0.684739	RRab; Bl	Y
Sz68	15.886111	-70.888826	15.492	0.331	0.917	0.474424	RRab; Bl	Y
Sz70	15.897164	-70.908059	19.025	0.456	0.633	0.583591	RRab	N
V002	15.840947	-70.905584	12.835	1.522	1.220	107.5510	LPV; RG	Y
LW03	15.806756	-70.843614	12.897	1.395	0.749	173.5635	LPV; RG	Y
LW08	15.887487	-70.827051	12.645	1.561	0.242	186.8250	LPV; RG	Y

[a] After C1-12.
[b] EA - detached eclipsing binary, EW - contact binary, Ell - Ellipsoidal variable, RRab - RRab pulsator, RRd - RRd pulsator.
[c] BS- blue straggler, RG - red giant, Bl - Blazhko effect.
[d] Membership status: Y - member, N - nonmember, U - no data or data ambiguous.

Table 5: Seasonal change of amplitudes in Sz55

	Ranges of (HJD-2450000)		
Freq.	1755–2135	3918–4362	4699–5128
f_0	0.520	0.378	0.319
$2f_0$	0.187	0.163	0.093
$3f_0$	0.226	0.112	0.054
$4f_0$	0.087	0.064	0.038[a]
$5f_0$	0.116	0.050	0.026

[a] $4f_0 - 1$ alias

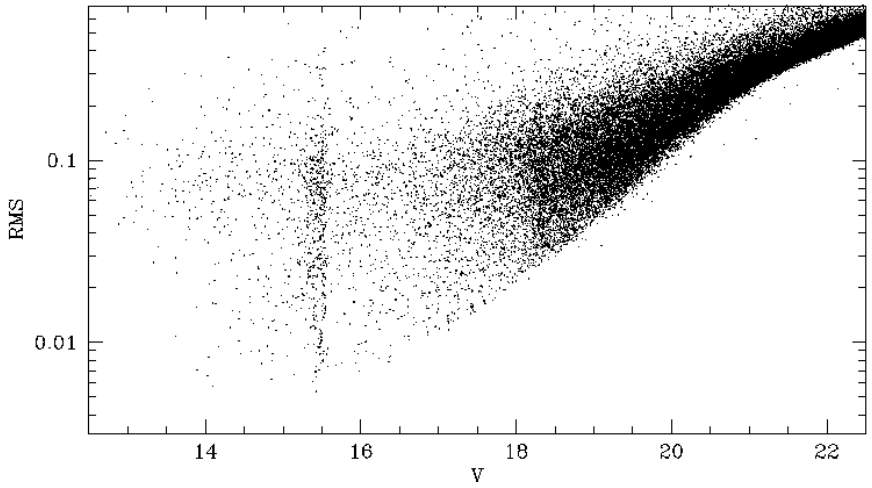

Figure 1: Standard deviation vs. average V magnitude for light curves of stars from the NGC 362 field.

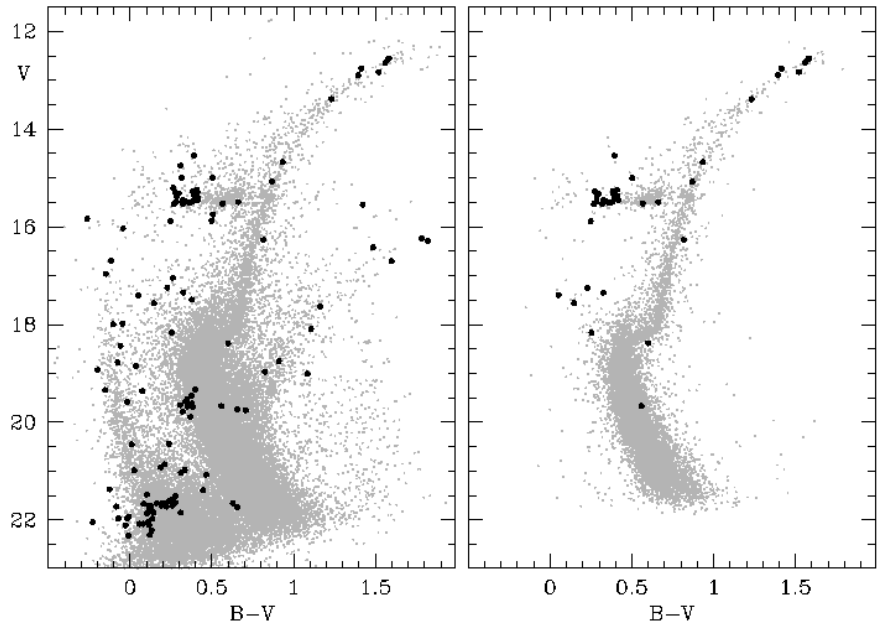

Figure 2: CMD for the observed field. Left: all stars for which proper motions were measured. Black points mark all the 138 variables detected within the present survey for which B-band magnitudes were available. Right: same as in the left frame, but for the PM-members of the cluster only.

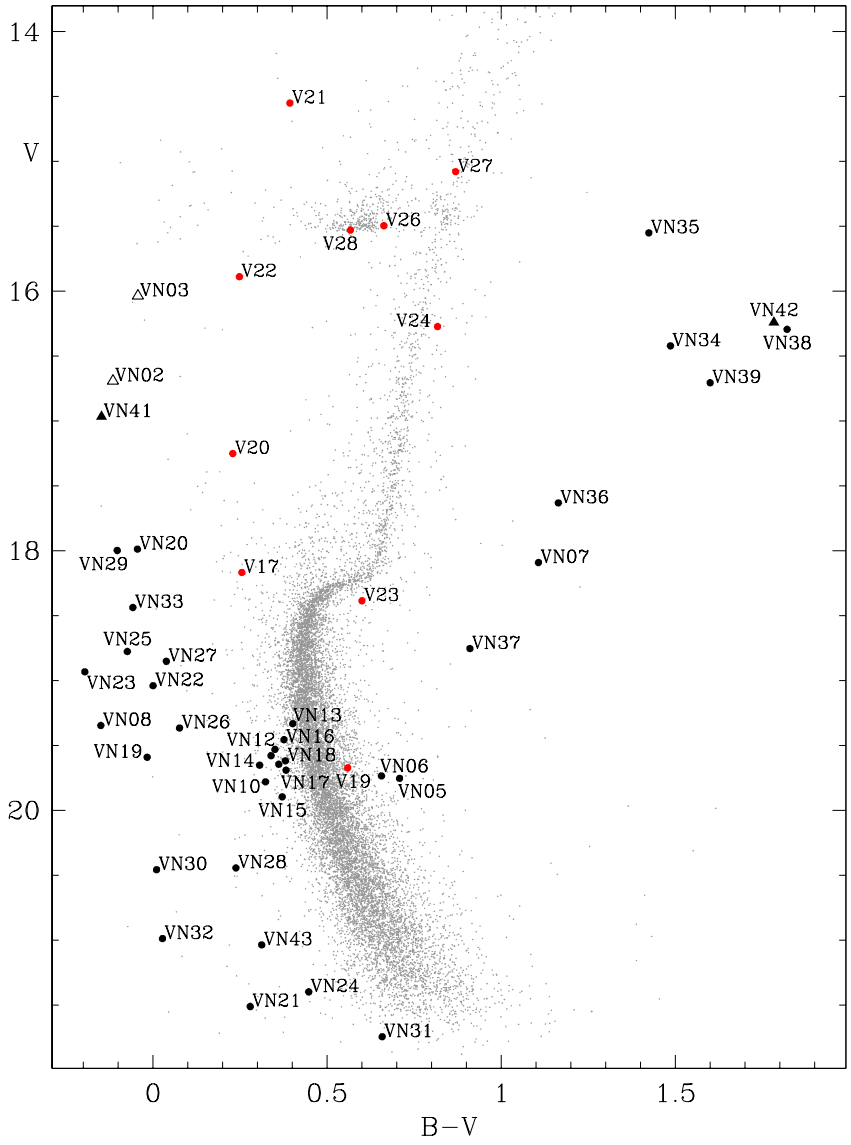

Figure 3: CMD for the observed field with locations of stars listed in Table 1 and Table 2. Circles: variable PM-members of the cluster (red) and variable field stars (black). Triangles: suspected variables (filled - field objects; open - objects for which the membership data is missing or ambiguous). The gray background stars are the same as in the right frame of Fig. 2.

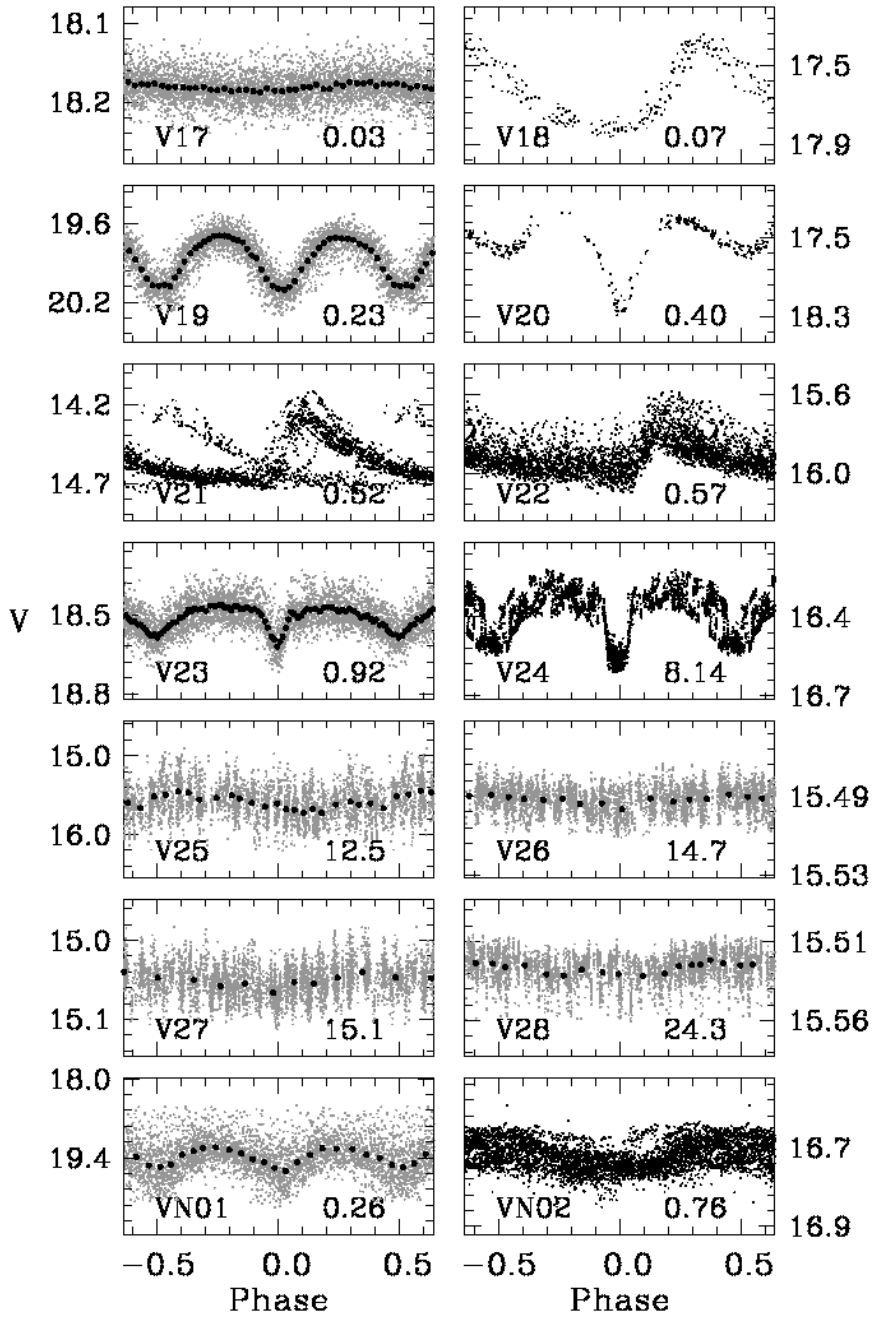

Figure 4a: Phased V-band light curves of the newly detected variables which are members or likely members of NGC 362. Phase-binned data are shown for selected stars with heavy black points. Individual panel labels give star ID and period in days.

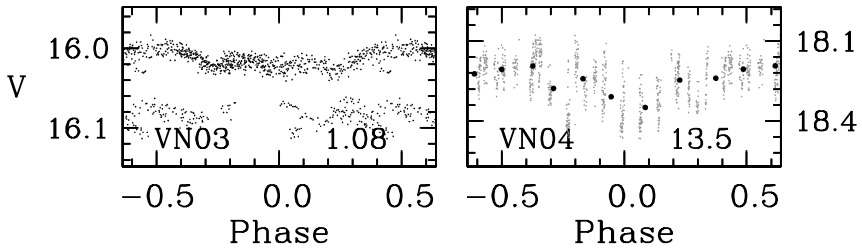

Figure 4b: Continuation of Fig. 4a.

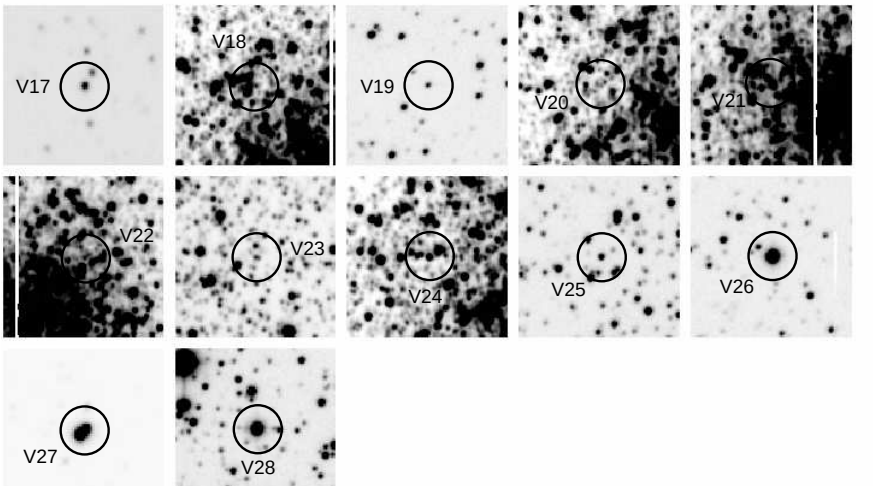

Figure 5: Finding charts for the new variable members of NGC 362. Each chart is 30″ on a side. North is up and East to the left.

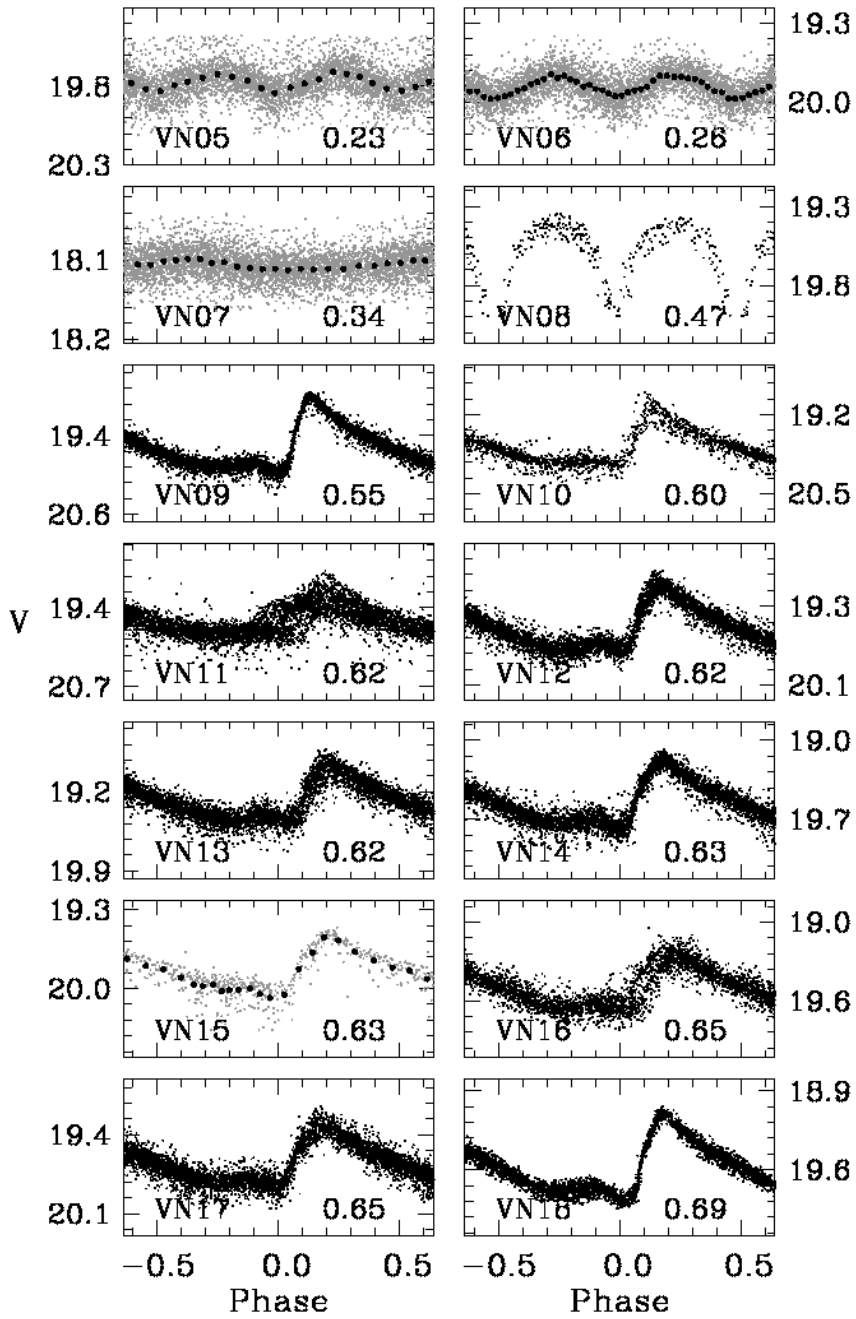

Figure 6a: Phased V-band light curves of stars listed in Table 2. Phase-binned data are shown for selected stars with heavy black points. Individual panel labels give star ID and period in days.

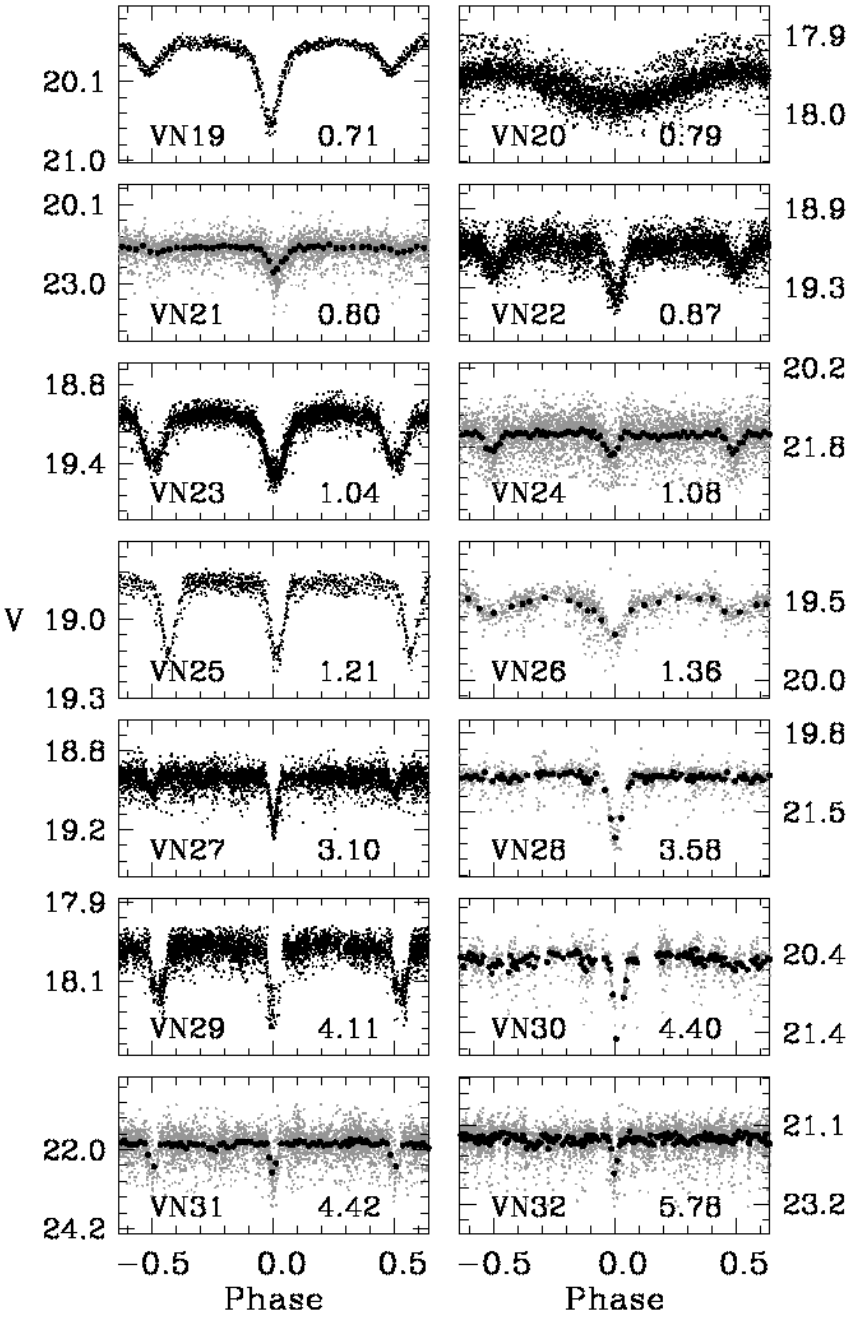

Figure 6b: Continuation of Fig. 6a.

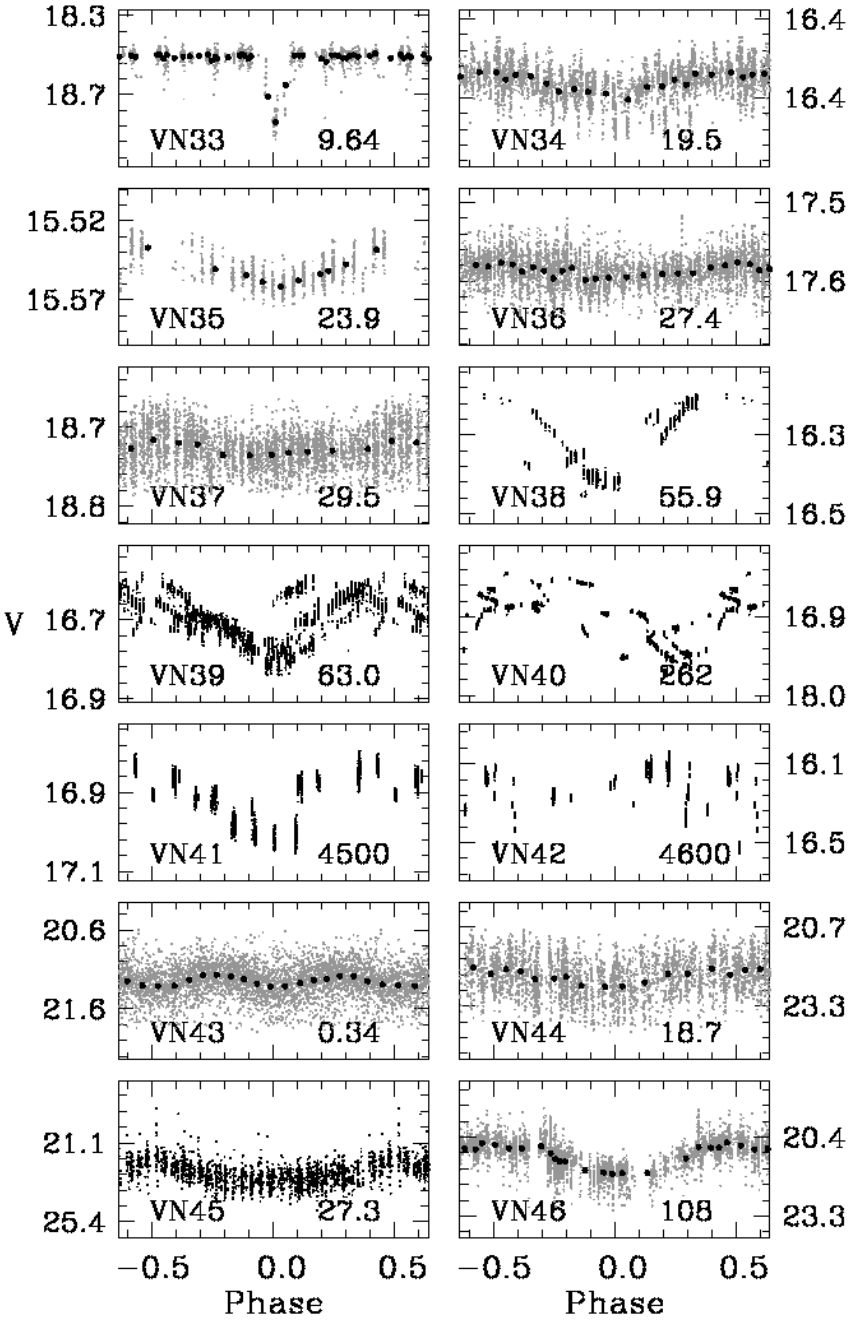

Figure 6c: Continuation of Fig. 6b.

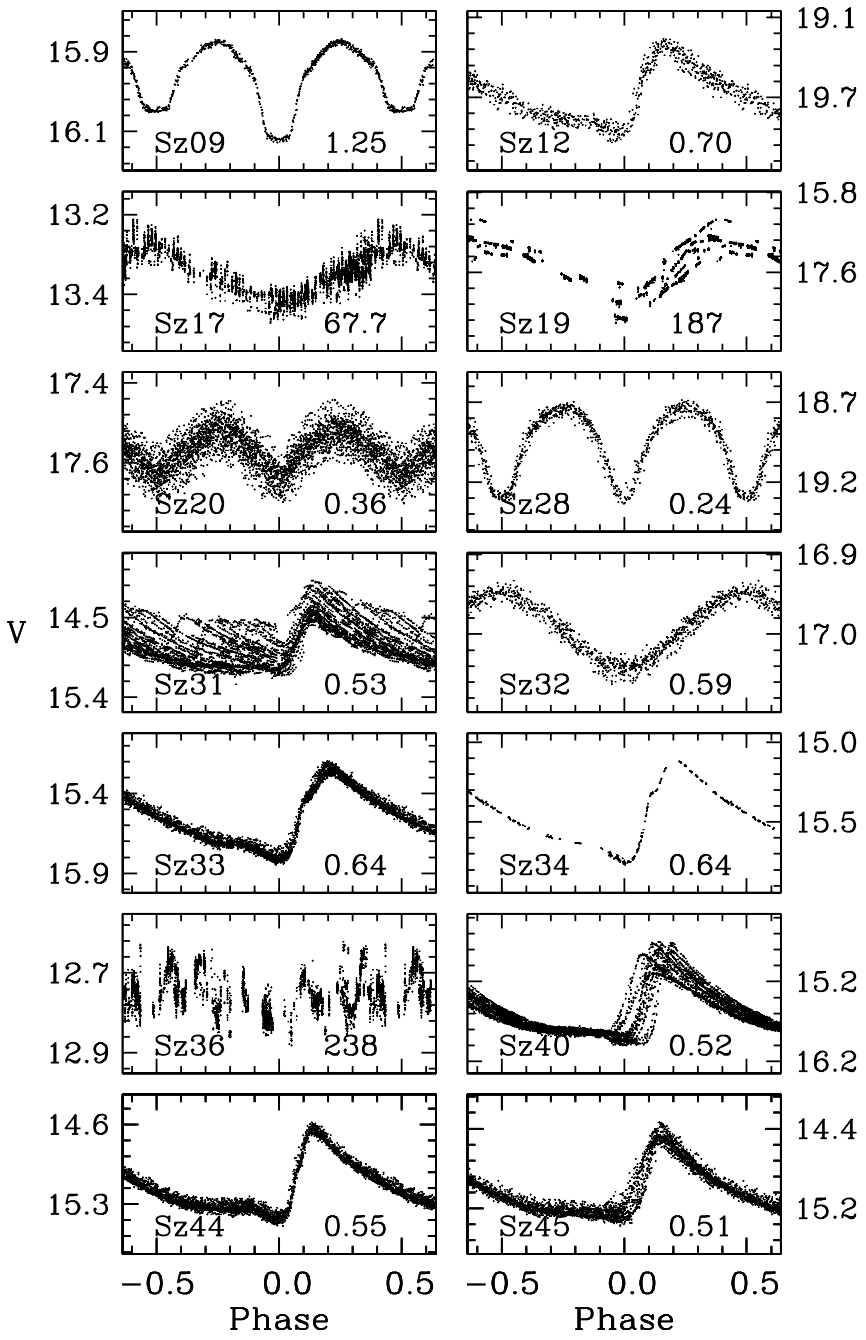

Figure 7a: Phased V-ligt curves of the S07 and LW11 variables listed in Table 4. Inserted labels give star ID and period in days.

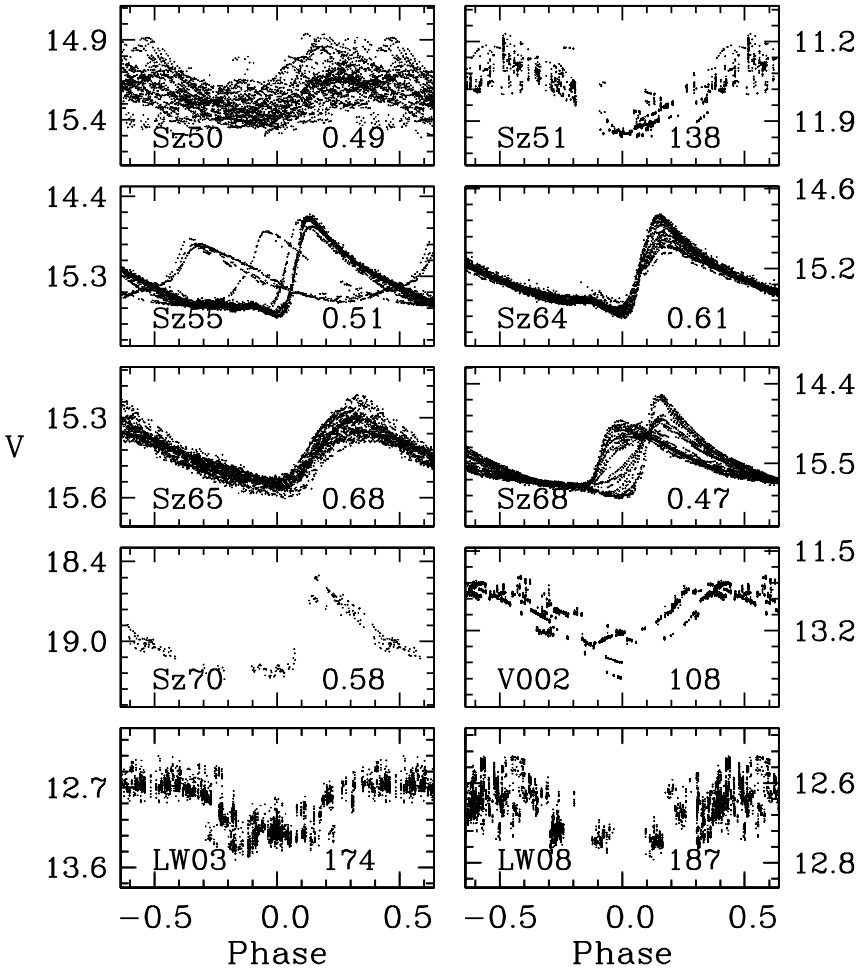

Figure 7b: Continuation of Fig. 7a.

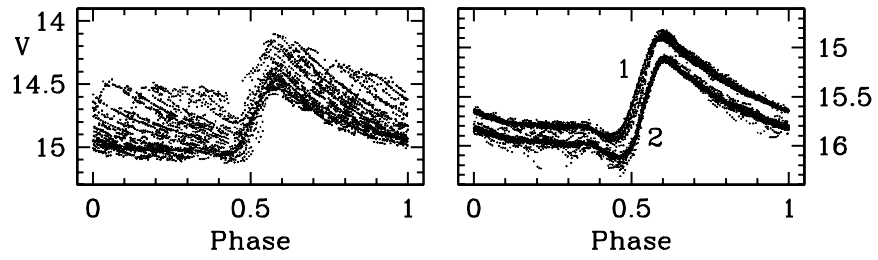

Figure 8: Left: the observed light curve of the Sz31 blend phased with $P = 0.530364$ d (same as in Fig. 7a). Right: disentangled light curves of the components of the blend phased with $P_1 = 0.530366$ d and $P_2 = 0.558817$ d. The curve #2 is shifted down by 0.2 mag for clarity.

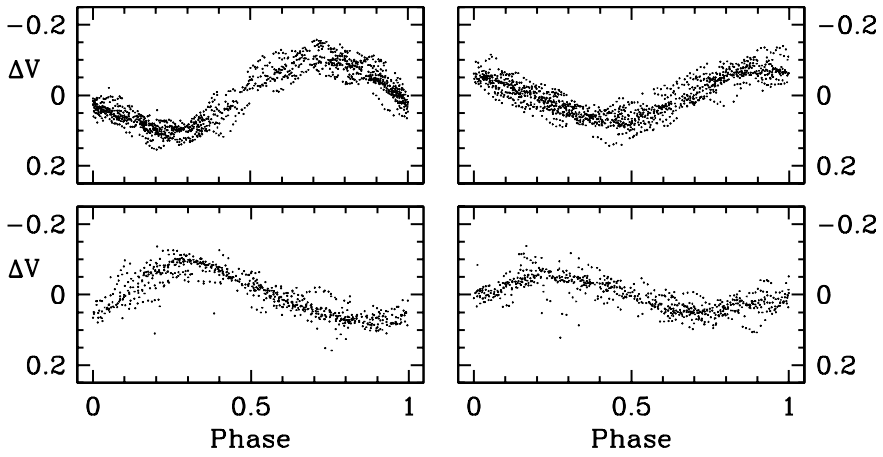

Figure 9: The light curve of Sz50 phased with frequencies f_0 and f_1 for Set 1 (upper left and right, respectively), and $2f_0$ and f_1 for Set 2 (lower left and right, respectively). In each case all other modes have been prewhitened.

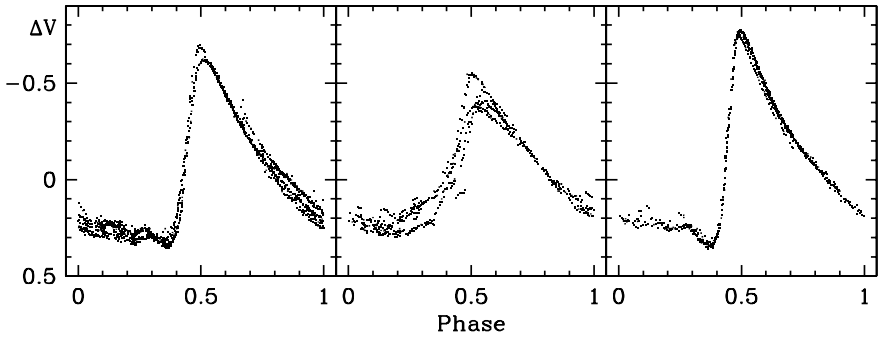

Figure 10: Seasonal changes of shape and amplitude of the Sz55 light curve. From left to right, the panels correspond to HJD ranges defined in Table 5. All curves are phased with the frequency f_0.